Geophysical Research Letters

RESEARCH LETTER
10.1029/2019GL084973

Increasing Water Vapor in the Stratosphere and Mesosphere After 2002

Jia Yue[1], James Russell III[1], Quan Gan[2], Tao Wang[3,4], Pingping Rong[1], Rolando Garcia[5], and Martin Mlynczak[6]

[1]Department of Atmospheric and Planetary Sciences, Hampton University, Hampton, VA, USA, [2]LASP, CU Boulder, Boulder, CO, USA, [3]University of Maryland, MD, JPL, NASA, CA, USA, [4]NASA Goddard Space Flight Center, Greenbelt, MD, JPL, NASA, CA, USA, [5]ACOM, NCAR, Boulder, CO, USA, [6]NASA Langley Research Center, Hampton, VA, USA

Key Points:
- SABER and MLS show a rapid global water vapor increase of 5-6% per decade in the lower stratosphere after 2002.
- SABER and MLS water vapor show positive trend and strong negative correlation with solar cycle in the mesosphere.
- SABER H2O time series and trend at 40N are consistent with the Boulder frost point hygrometer measurements after 2002.

Correspondence to:
J. Yue,
yuejia1979@gmail.com

Citation:
Yue, J., Russell, J., III, Gan, Q., Wang, T., Rong, P., Garcia, R., & Mlynczak, M. (2019). Increasing Water Vapor in the Stratosphere and Mesosphere After 2002. *Geophysical Research Letters*, *46*. https://doi.org/10.1029/2019GL084973

Received 12 AUG 2019
Accepted 3 NOV 2019
Accepted article online 9 NOV 2019

Abstract Water vapor (H_2O) measurements made by the Sounding of the Atmosphere using Broadband Emission Radiometry (SABER) instrument between 2002 and 2018 and by the Aura Microwave Limb Sounder (MLS) instrument between 2004 and 2018 are analyzed to determine the linear trend and solar cycle response of H_2O in the stratosphere and mesosphere. Both SABER and MLS show a rapid global H_2O increase of 5–6% per decade in the lower stratosphere after the 2001 drop. The increasing zonal mean H_2O at 40°N in SABER and MLS is consistent with the Boulder frost point hygrometer data in the lower stratosphere. The global distribution of SABER and MLS H_2O trends are positive at most altitudes and latitudes, and they peak in the tropical lower stratosphere. In the mesosphere the SABER H_2O trend is 0.1–0.2 ppmv per decade and the MLS H_2O trend is 0.2–0.3 ppmv per decade. The trend and solar cycle response derived from the observations are compared against the Whole Atmosphere Community Climate Model (WACCM). The solar cycle response of H_2O from WACCM agrees with SABER and MLS. The linear H_2O trend from WACCM does not show the observed increase in the lower stratosphere.

1. Introduction

Water vapor (H_2O) is a key trace gas throughout the Earth's atmosphere. It fundamentally regulates the weather and climate of our planet (Brasseur & Solomon, 1995; Wallace & Hobbs, 2006). Water vapor in the stratosphere originates from both transport of tropospheric air through the tropical tropopause (Brewer, 1949) and in situ methane oxidation in the middle to upper stratosphere (Jones et al., 1986). Increasing stratospheric water vapor, especially in the lower stratosphere, cools the stratosphere but warms the troposphere (Dessler et al., 2013; Foster & Shine, 1999; Oinas et al., 2001; Shindell, 2001; Smith et al., 2001; Solomon et al., 2010). Accordingly, the 10% decrease of stratospheric water vapor right after 2000 (Randel et al., 2006) could have slowed the rate of global surface temperature increase by about 25% (Solomon et al., 2010). Increased water vapor in the stratosphere can also enhance polar stratospheric cloud formation and lead to more prolonged high-latitude ozone loss (Kirk-Davidoff et al., 1999; Shindell, 2001; Forster and Shine, 1999). In the upper mesosphere, more abundant water vapor from increasing methane contributes to more frequent polar mesospheric cloud occurrences at ~82 km (Thomas et al., 1989; Lubken et al., 2018). Based on all the mechanisms above, we argue that a long-term increase or decrease of water vapor in the stratosphere and mesosphere will have fundamental global and regional impacts.

Using the water vapor measurements obtained from balloon-borne frost point hygrometers (FPH) launched from Boulder, Colorado (40°N, 105°W), Oltmans and Hofmann (1995) and Oltmans et al. (2000) estimated about 1–1.5%/year increase from 14 to 28 km during 1965–2000. Using the same FPH data from 1980 to 2010, Hurst et al. (2011) showed that stratospheric water vapor increased water vapor during 1980–2010 despite significant short-term variability, decreased during 2001–2005 (the abrupt "drop" described by Solomon et al., 2010), and then increased again during 2006–2010. In contrast to the FPH measurements, the Halogen Occultation Experiment (HALOE) lower stratosphere water vapor over 1992–2003 shows a relatively constant or even decreasing trend (Randel et al., 2004). Strong correlations were found between the lower stratospheric H_2O and tropical tropopause temperatures, especially the cold point tropopause temperature. No clear trends are identified in the cold point tropopause temperature in Randel et al. (2004). Merging multiple satellite datasets starting from 1988, Hegglin et al. (2014) determined that global lower stratospheric water vapor trends are slightly negative, agreeing with the HALOE analysis. Dessler et al.

(2014) showed that the variations in water vapor can be largely explained by dynamical factors such as the quasi-biennial oscillation (QBO), the Brewer-Dobson circulation (BDC), and temperature changes at 500 hPa (Dessler et al., 2013). Since there is no consensus that a significant long-term trend has occurred in the amount of water vapor entering the stratosphere through the tropical tropopause, many questions remain open concerning whether the stratospheric water vapor trend ever existed, how these trends vary with latitude and altitude, or how to interpret the discrepancies between different measurements and the possible mechanisms.

There have been fewer observations of water vapor in the mesosphere. Using ground-based water vapor millimeter-wave spectrometer and satellite measurements, Nedoluha et al. (2013) found that H_2O has been increasing in the lower mesosphere since 2006. Remsberg et al. (2018) also reported a positive linear trend of HALOE water vapor in the midlatitude mesosphere. To gain a better understanding of the mesospheric water vapor, more studies are needed.

In this paper, we will analyze the linear trend and solar cycle response in the newly retrieved Sounding of the Atmosphere using Broadband Emission Radiometry (SABER) H_2O in the stratosphere and mesosphere from 2002 to 2017 and compare these findings with the Aura Microwave Limb Sounder (MLS) H_2O results from 2004 to 2017. This paper assumes that SABER and MLS instruments are stable that their systematic errors have not significantly changed.

2. Observations

The SABER instrument on the Thermosphere-Ionosphere-Mesosphere Energetics and Dynamics (TIMED) satellite was launched on 7 December 2001. SABER measures vertical profiles of infrared limb radiance in 10 broadband spectral channels with band centers ranging from ~1.6 to 17 μm. Profiles are sampled at 0.35-km intervals with a 2-km vertical field of view (Russell et al., 1999). The profiles obtained in both the ascending and descending portions of the TIMED orbit, corresponding to two local times every day. SABER radiances are used to retrieve altitude profiles of temperature and volume mixing ratios of Earth atmosphere minor species (i.e., CO_2, O_3, H_2O, [O], and [H]) in the altitude range of ~15–110 km depending on channel. Other parameters used to characterize the energetics in the MLT region are also retrieved. Continuous latitude coverage is provided ranging from 53°S to 83°N switching to the 83°S to 53°N every ~60 days, as the TIMED spacecraft rotates 180° about its yaw axis (Russell et al., 1999). SABER has a local time precession of 12 min/day and it takes ~60 days to sample all local times with fairly uniform local time steps and remove tidal aliasing. The instrument has been operating nominally since January 2002. No major SABER data gaps (100% duty cycle) existed within 53°S–53°N.

SABER version 2.07 H_2O mixing ratio from ~100 hPa (~16 km) to 0.006 hPa (~83 km) is retrieved from the 6.8-μm channel (Rong et al., 2019). The long-standing positive bias caused by spectral out-of-band emission in the H_2O channel due to O_3 has been corrected in version 2.07 data that are now publicly available. The data were also screened using a threshold of 12 ppmv in the 25–80 km range. A 12 ppmv is based on several other data sets such as Atmospheric Chemistry Experiment (ACE) and MLS. ACE can reach 13–14 ppmv occasionally, whereas MLS H_2O can exceed 11–12 ppmv. Detailed discussions of screening are presented in Rong et al. (2019). SABER H_2O has a vertical resolution of 2 km throughout the altitude range from the tropopause to ~80 km. Table 1 of Rong et al. (2019) provides the itemized and total error analysis. Single-profile random errors are ~2–3% up to 60 km and increase rapidly to 30% at 80 km due to degraded signal-to-noise ratio in the radiance measurement. The total systematic error (10–20%) increases toward both the lower and upper ends of the altitude range caused by temperature and nonlocal thermal equilibrium effects, respectively.

The MLS instrument on the Aura satellite was launched on 15 July 2004. The Aura satellite orbit is sun synchronous with a 98° inclination and 705-km altitude. MLS scans Earth's limb from the surface to 90 km globally from 82°S to 82°N (Waters et al., 2006). The MLS H_2O product is retrieved from its 190-GHz band at both ascending and descending orbits (Lambert et al., 2007). The current v4.2 MLS H_2O has a vertical resolution of ~3 km below ~50 km and degrades to ~10 km at ~83 km. Single-profile random errors range from 15% near the tropopause, to 6% in the stratosphere, and up to 55% near 80 km altitude. The MLS v4.2 H_2O systematic error varies in the range of ~5–19% below ~75 km and exceeds 20% above ~83 km.

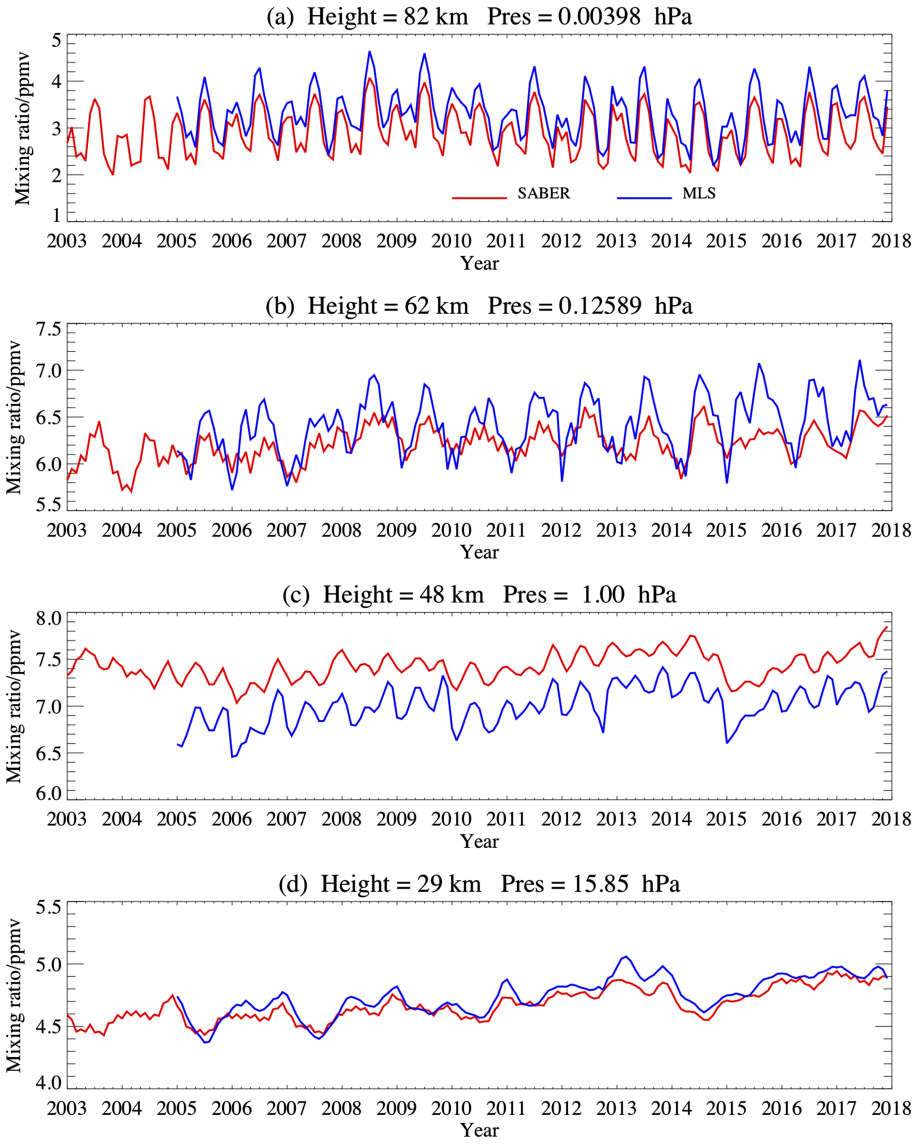

Figure 1. Time series of bimonthly global mean (55°S–55°N) SABER (red) and MLS (blue) H_2O mixing ratio (a) 82, (b) 62, (c) 48, and (d) 29 km.

Figure 1 displays the global (55°N–55°S) bimonthly running mean time series of H_2O mixing ratio from SABER and MLS in the stratosphere and mesosphere after 2002. The tidal effect or local time variation of SABER H_2O is largely removed with the 60-day or yaw cycle average. SABER and MLS H_2O are generally in good agreement except at 48 km where SABER H_2O is about 0.5 ppmv higher than MLS systematically after being averaged globally. This is overall consistent with the multiyear average shown in Rong et al. (2019) indicating that, around the stratopause, SABER H_2O is persistently higher than MLS H_2O. Seasonal variations of H_2O have been discussed in the profile comparisons of Rong et al. (2019) and references therein, thus will not be repeated here. It is clear that during the early 2000s the stratospheric H_2O was recovering from the well-known sudden drop in 2001 (Randel et al., 2006; Solomon et al., 2010). There was another H_2O drop in the stratosphere around 2014–2015. At 29 km, both SABER and MLS H_2O increased steadily from ~4.4–4.7 ppmv in 2003–2005 to ~4.9 ppmv in 2018. In the mesopause region (~82 km), the interannual behavior of H_2O is largely controlled by photolysis, which produces OH and H, exhibiting a variation pattern in concert with the solar cycle. It is apparent that H_2O at 82 km was more abundant during solar minimum, around 2009.

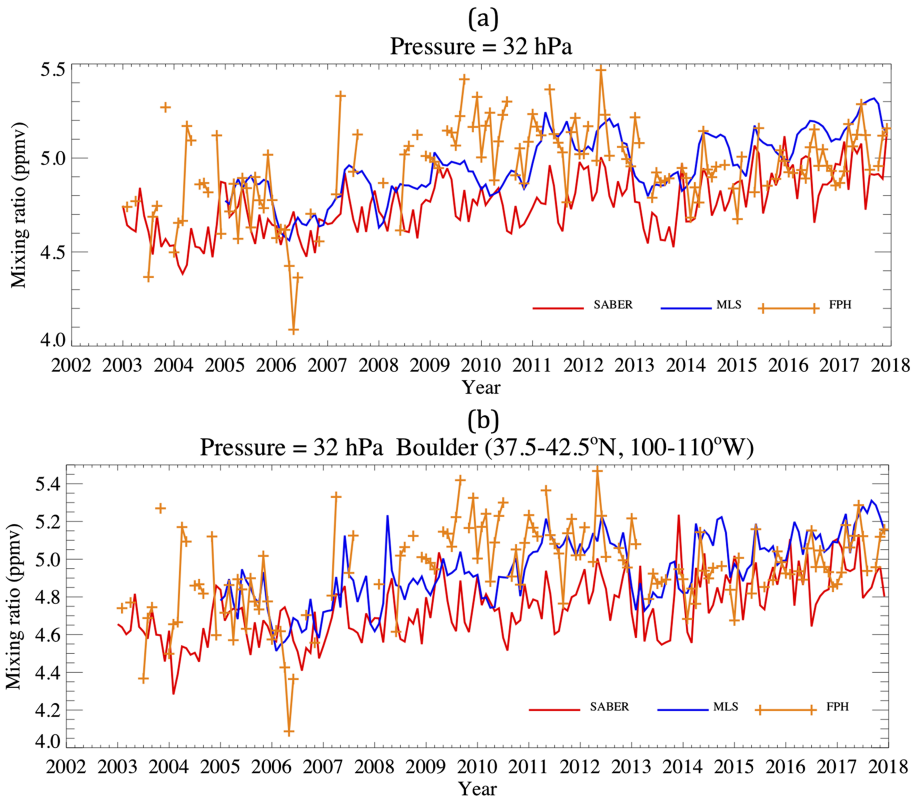

Figure 2. Time series of (a) monthly zonal mean SABER (red) and MLS (blue) H_2O mixing ratio at 32 hPa and 40°N and (b) corresponding SABER and MLS H_2O mixing ratio near Boulder (37.5–42.5°N, 100–110°W), compared with the Boulder NOAA frost point hygrometer measurement (orange pluses).

The Boulder FPH data obtained since April 1980 is the longest running stratospheric H_2O measurement (Hurst et al., 2011, 2016). However, it is debatable whether the long-term H_2O increase indicated by the FPH is representative of the global water vapor trend, as it is not continuous and from a single point. The lower stratosphere H_2O from a merged satellite data set (HALOE, SAGEII, ACE-FTS, Aura-MLS, SMR, and MIPAS) actually shows a negative trend during 1986–2010 (Hegglin et al., 2014). Lossow et al. (2018) suggest that the differences in the data sampling (Boulder at ~40°N, 105°W vs. the zonal mean) cannot explain the trend discrepancy between the FPH measurements and the zonal mean satellite data in 1980–2010. Figure 2 compares the Boulder FPH measurements with the monthly zonal mean time series (Figure 2a) of both SABER and MLS H_2O at 40°N and 32 hPa and the counterparts near Boulder (±2.5° latitude and ±5°longitude) (Figure 2b). It is clear that the zonal mean is representative of the atmosphere over Boulder. Although the FPH measurements (orange plus signs) have larger variability, the overall increasing H_2O amount after 2002 is in general consistent among these three data sets. The zonal mean long-term trends at 40°N are 0.20±0.04 ppmv/decade, 0.23±0.01 ppmv/decade, and 0.39±0.01 ppmv/decade for FPH, SABER, and MLS, respectively. In particular, SABER and the FPH measurement agree very well since 2014. Nevertheless, the FPH measurements and the zonal mean satellite data during 2002–2017 display similar H_2O trends.

We applied the same multiple linear regression (MLR) method used in Yue et al. (2015) to the SABER (2003–2017) and MLS (2005–2017) bimonthly mean H_2O time series and calculated the global mean (±55° for both MLS and SABER) H_2O linear trend and solar cycle responses with 2σ uncertainties, as illustrated in Figure 3. The MLR uncertainties depend on the scatter of the time series and their autocorrelation (Yue et al., 2015). The annual oscillation, semi-annual oscillation, QBO, and El Nino-Southern Oscillation terms were also fitted in the MLR (not shown) and removed. The indices of solar cycle (F10.7), QBO, and El Nino-Southern Oscillation used in the regression were introduced in Yue et al. (2015). In a test, we compared the trends of SABER H_2O for 2003–2017 and 2005–2017, and they are almost identical, indicating that

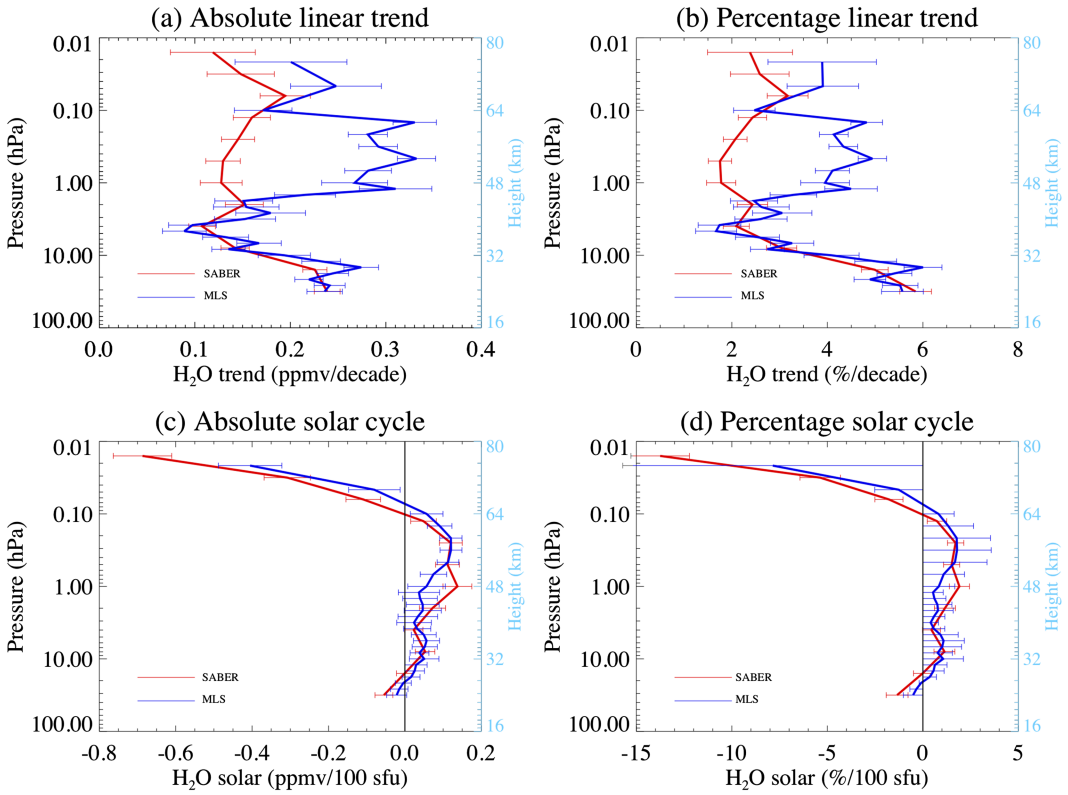

Figure 3. Global mean water vapor mixing ratio absolute and relative linear trend and solar cycle response for SABER (red, 2002–2017) and MLS (blue, 2004–2017). The relative trend is defined as the absolute value divided by the multi-year mean H_2O profiles. The uncertainty denotes the 95% confidence level.

the trend is not sensitive to the 2002–2004 period. This indicates that the 2-years shorter MLS time series does not constitute a problem for the present trend study. The linear trends of both SABER and MLS in Figure 3 are large in the lower stratosphere below 10 hPa, that is, about 5–6% (or 0.25 ppmv) per decade at 30 hPa (~25 km). This is half of the FPH H_2O trend magnitude in Boulder between 1980 and 2010 (13.5% or 0.5 ppmv per decade) (Hurst et al., 2011) but much larger than (and of opposite sign to) the negative trend derived from the merged satellite observations (Hegglin et al., 2014). In the upper stratosphere and mesosphere, the SABER H_2O trend of 2–3% or 0.1–0.2 ppmv per decade is smaller than that of MLS (3–4.5% or 0.2–0.3 ppmv per decade).

In the mesosphere, complete methane oxidation is a major source of water vapor (Brasseur & Solomon, 1995). One can estimate the H_2O trend due purely to increasing CH_4 by assuming complete methane oxidation in the upper stratosphere/lower mesosphere (i.e., loss of one CH_4 molecule produces two H_2O molecules) and using the observed global surface methane estimated to have increased from about 1.77 ppmv in 2000 to 1.82 ppmv in 2015 or about 0.035 ppmv per decade (https://www.esrl.noaa.gov/gmd/ccgg/trends_ch4/#global_growth). This corresponds to 0.07 ppmv per decade for the H_2O trend assuming that all of the CH_4 is oxidized into H_2O in the mesosphere above 0.1 hPa (i.e., above ~65 km). Even so, the contribution of increasing methane oxidation to the H_2O trend is only able to explain ~50% of the SABER H_2O trend of 0.1–0.2 ppmv per decade above 0.1 hPa. The rest of the observed H_2O trend is attributed to the behavior of H_2O transported from below.

On the other hand, the solar cycle response of H_2O in Figure 3 is very consistent between SABER and MLS in the mesosphere. Because of stronger photodissociation of H_2O during solar maximum, variations of H_2O and F10.7 show increasingly negative correlation at higher altitudes (Figure 3). Interestingly, there is a small positive correlation between H_2O and the solar cycle in the stratosphere that cannot be explained by chemistry alone. Solar cycle variations of dynamics and transport could contribute to this position correlation. We will investigate this feature together with modeling studies in the future.

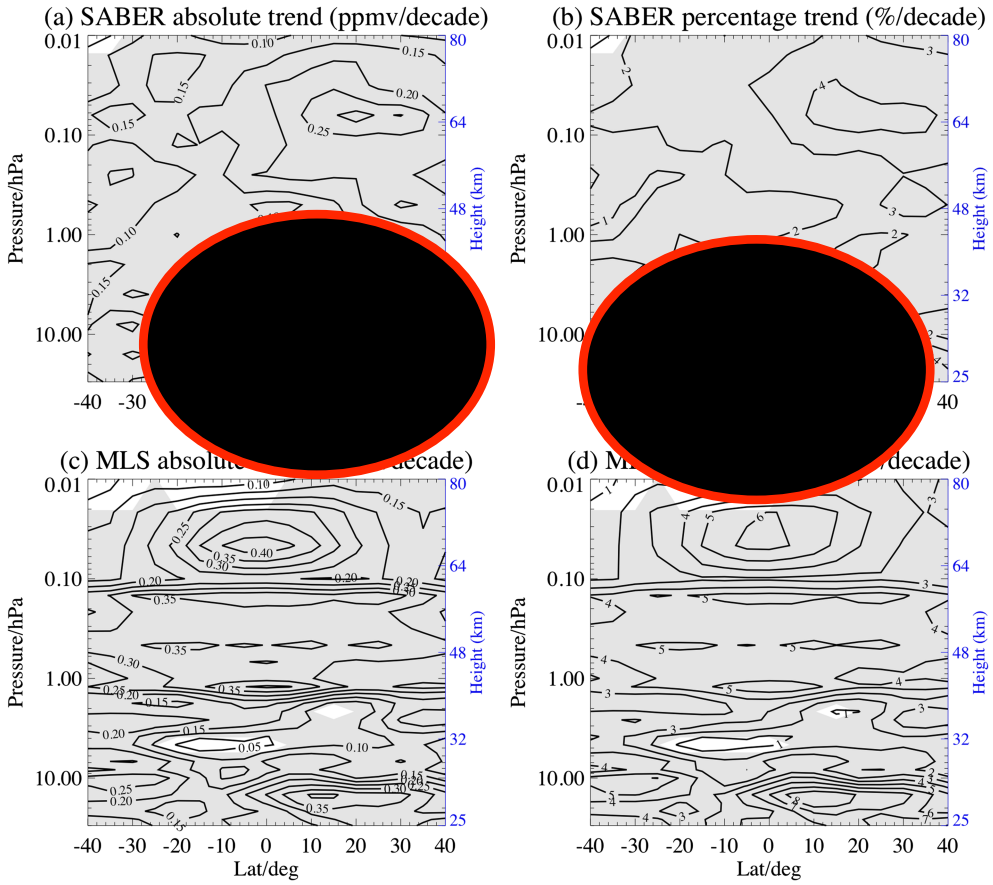

Figure 4. SABER (a) H_2O absolute (ppmv per decade) and (b) relative trends (% per decade) and MLS (c) H_2O absolute (ppmv per decade) and (d) relative trends (% per decade) as a function of latitude andpressure. Shaded area denotes the significance results under the 2σ uncertainty.

Figure 4 shows the global distribution of SABER and MLS H_2O linear trends. The SABER linear trends are as large as 7% per decade in the tropical lower stratosphere and become smaller at higher latitudes. Such a large trend in the tropical lower stratosphere is consistent with the notion that H_2O enters the lower stratosphere from the tropical tropopause (e.g., Dessler et al., 2014) with mixing ratio controlled by the tropopause cold point. In the lower stratosphere, the upwelling branch of the BDC transports tropical H_2O to higher altitudes and latitudes. The acceleration of the BDC due to increasing greenhouse gasses [see, e.g., Garcia & Randel, 2008] and increased water vapor injection into the stratosphere due to increasing penetration of overshooting tops (Anderson et al., 2018) can further influence the H_2O trend in the stratosphere. The MLS H_2O trend in the stratosphere shows a more complex structure compared to SABER. In the mesosphere, both the latitudinal distributions and the magnitudes of the trends differ between the two analyses, that is, the MLS H_2O trend shows a larger value of 6% per decade between 0.1 hPa and 0.01 hPa, while the SABER H_2O trend is at a maximum of 4% per decade. In addition, the MLS H_2O trend exhibits larger values centered in the equatorial region, whereas the SABER trend maximum is located in the northern hemisphere. Although SABER is free from tidal aliasing, MLS only measures two local times each day. It is sufficient to remove diurnal tidal aliasing with ascending and descending observations averaged; however, semidiurnal tidal aliasing may still not be completely removed.

3. Discussion and Summary

This paper presents the global H_2O trend from a newly developed SABER data set. SABER contains the longest single satellite record of H_2O in the stratosphere and mesosphere (2002 until present). The number of H_2O profiles retrieved from SABER and MLS is much larger than previous missions such as HALOE and

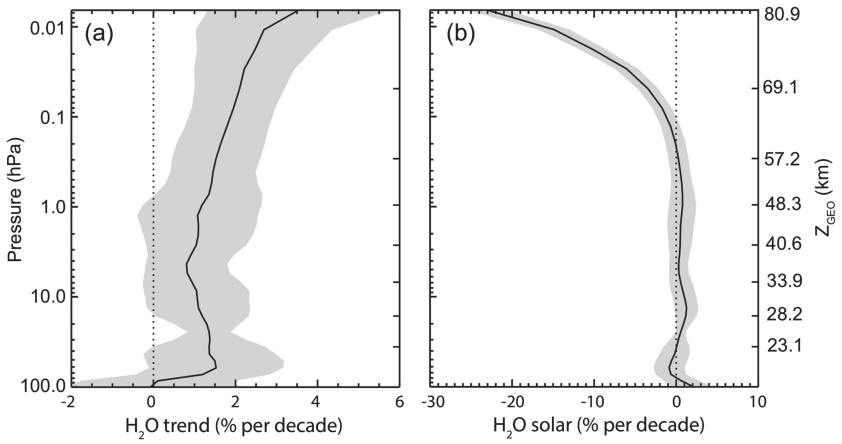

Figure 5. Relative (a) linear trend and (b) solar cycle response of global mean WACCM H_2O from 2002 to 2015. Shaded area is significant at 95%.

SAGE II (most of which used solar occultation and therefore provided much sparser coverage). Thus, the calculated global H_2O trend from limb emission measurements during 2003–2017 has a greater statistical significance because on the order of ~1,500 H_2O profiles are measured each day by, for example, SABER, versus only 30 per day for the occultation measurements. The increasing trends of zonal mean MLS and SABER H_2O at 40°N are consistent with what is shown in the Boulder FPH data in the lower stratosphere (at 32 hPa, see Figure 2). The global distributions of SABER and MLS H_2O trends both peak in the tropical lower stratosphere and show a similar rapid global H_2O increase of 5–6% per decade in that altitude range. We earlier discussed the idea in connection with Figure 4 that this behavior could be driven by the BDC. In the mesosphere, the MLS H_2O trend of 0.2–0.3 ppmv per decade is much greater than the SABER trend of 0.1–0.2 ppmv per decade.

In an attempt to shed further light on the lower stratosphere H2O increase, Figure 5 shows the simulated linear trend and solar cycle response from a WACCM Chemistry-Climate Model Initiative REFC1 simulation during the 2002–2015 period. In this simulation, the model is free running, but not coupled to the ocean, since the sea surface temperatures is specified from observations. Between 10 and 0.1 hPa, WACCM and SABER H2O trends are consistent at ~2% per decade. On the other hand, the large H_2O trend in the lower stratosphere observed by SABER and MLS was not reproduced in WACCM. This might suggest that a physical mechanism responsible for this large H_2O increase is absent in the model. According to Dessler et al. (2014), the QBO, the strength of the BDC, or the temperature of the tropical troposphere all can affect how much water vapor enters the stratosphere through the tropical tropopause. The question whether these three processes are accurately represented in WACCM or if any of the individual processes is dominant will be examined in a follow-up paper. Meanwhile, it is encouraging that the solar cycle response in H_2O is consistent between WACCM and the observations, which shows a negative response in the mesosphere. This suggests that photodissociation of H_2O is well represented in WACCM.

The SABER H_2O record is still shorter than two solar cycles given its ~17.5 years of coverage thus far. It is also much shorter than the Boulder FPH data record (1980–present) (Hurst et al., 2011) and merged satellite data sets (1985–2010) (Hegglin et al., 2014). Therefore, we cannot rule out the possibility that longer term natural variability could be responsible for the seemingly large H_2O trend in the SABER analysis (e.g., Dessler et al., 2014; Hegglin et al., 2014), especially since the time series began right after the 2001 H_2O decrease. We hope to revisit this H_2O long-term trend with longer records from SABER or MLS in the future. Currently, both instruments are functioning well. The high consistency between the SABER and MLS H_2O at 40°N and Boulder FPH measurements after 2003 lends additional confidence to the increasing trend since 1980 reported in Hurst et al. (2011). At least after 2003, the Boulder FPH measurement is consistent with the zonal mean at 40°N and even the global trend. We have no answers as to why the merged satellite H_2O trend is so different from the Boulder FPH measurement (Hegglin et al., 2014). One thing to be checked is whether

the asynoptic sampling in the earlier satellite solar occultation observations have caused an artificial H_2O trend over the years, such as in HALOE or SAGE II.

The increasing global H_2O throughout the stratosphere and mesosphere shown in Figure 4 has potentially important impacts on climate, chemistry, and aeronomy. Solomon et al. (2010) argued that the stratospheric water vapor increase of about 1 ppmv from 1980 to 2000 could account for 0.24 W/m^2 radiative forcing. By comparison, SABER and MLS detected about a 0.45 ppmv increase from 2003 to 2017. Thus, the radiative forcing due to this H_2O increase is not negligible for surface global warming. It is known that increasing H_2O also leads to ozone depletion [e.g., Sindell, 2001]. The strong H_2O trend observed by SABER and MLS since 2003 could possibly interfere with the healing of the ozone hole that has occurred since 2000 (Solomon et al., 2016). These water vapor increases might not be true secular trends but could instead be due to random, low frequency natural variability. The uncertain natural variability can result in incorrect trends. On the other hand, any trend in the stratosphere or mesosphere due to CH_4 is a long-term trend, driven by anthropogenic increases in CH_4. Lübken et al. (2018) have demonstrated that the more frequent appearance of noctilucent clouds at ~83 km since the 1800s was mainly driven by the increase in water vapor due to methane oxidation in the mesosphere, as opposed to other factors, such as a colder mesopause temperature. The increasing mesospheric H_2O seen in SABER and MLS since 2003 supports the conclusion in Lübken et al. (2018). The overall impacts of H_2O changes in the stratosphere and mesosphere observed by SABER and MLS in the 21st century will be quantified in future focused studies.

Acknowledgments
JY thanks Susan Solomon, Bill Randel, and Mark Schoeberl for helpful discussions about the H_2O trend and Dong Wu and Jae Lee for information about the MLS data. We would also like to acknowledge the hard work and support of the SABER retrieval team, who provided the version 2.0 data, including scientists from GATS, Inc., NASA Langley Research Center, NASA Goddard Space Flight Center, Instituto de Astrofísica de Andalucía (Spain), and Arcon, Inc. J. Y. and J. R. were supported by NSF AGS-1901126. J. Y. was supported by NASA 80NSSC19K0835 and NNH18ZDA001N-HGIO. The SABER H_2O data can be downloaded at http://saber.gats-inc.com/data_services.php. We would also like to thank the MLS team for providing the H_2O v4.2 data: https://mls.jpl.nasa.gov/products/h2o_product.php. The National Center for Atmospheric Research is sponsored by the National Science Foundation. The WACCM CCMI outputs can be accessed at https://www2.acom.ucar.edu/gcm/ccmi-output. The authors thank the two reviewers for their constructive comments.

References

Anderson, J. G., Wilmouth, D. M., Smith, J. B., & Sayres, D. S. (2018). UV Dosage levels in summer: Increased risk of ozone loss from convectively injected water vapor. *Science*, *337*, 825–839.

Brasseur, G., & Solomon, S. (1995). *Aeronomy of the middle atmosphere, D*. Dordrecht/Boston/Lancaster: Springer.

Brewer, A. W. (1949). Evidence of a world circulation provided by measurements of helium and water vapor distribution in the stratosphere. *Quart. J. Roy. Meteor. Soc.*, *75*, 351–363.

Dessler, A. E., Schoeberl, M. R., Wang, T., Davis, S. M., & Rosenlof, K. H. (2013). Stratospheric water vapor feedback. *P. Natl. Acad. Sci. USA*, *110*(45), 18087–18091. https://doi.org/10.1073/pnas.1310344110

Dessler, A. E., Schoeberl, M. R., Wang, T., Davis, S. M., Rosenlof, K. H., & Vernier, J.-P. (2014). Variations of stratospheric water vapor over the past three decades. *Journal of Geophysical Research: Atmospheres*, *119*, 12,588–12,598. https://doi.org/10.1002/2014JD021712

Foster, P. M., & Shine, K. P. (1999). Stratospheric water vapor changes as a possible contributor to observed stratospheric cooling. *Geophysical Research Letters*, *26*(21), 3309–3312.

Garcia, R., & Randel, W. (2008). Acceleration of the Brewer-Dobson circulation due to increases in greenhouse gases. *Journal of the Atmospheric Sciences*, *2731-2739*.

Hegglin, M. I., et al. (2014). Vertical structure of stratospheric water vapour trends derived from merged satellite data. *Nature Geoscience*. https://doi.org/10.1038/NGEO2236

Hurst, D. F., Oltmans, S. J., Vömel, H., Rosenlof, K. H., Davis, S. M., Ray, E. A., et al. (2011). Stratospheric water vapor trends over Boulder, Colorado: Analysis of the 30 year Boulder record. *Journal of Geophysical Research*, *116*, D02306. https://doi.org/10.1029/2010JD015065

Hurst, D. F., Read, W. G., Vömel, H., Selkirk, H. B., Rosenlof, K. H., Davis, S. M., et al. (2016). Recent divergences in stratospheric water vapor measurements by frost point hygrometers and the Aura Microwave Limb Sounder. *Atmospheric Measurement Techniques*, *9*(9), 4447–4457. https://doi.org/10.5194/amt-9-4447-2016

Jones, R. L., Pyle, J. A., Harries, J. E., Zavody, A. M., Russell, J. M., & Gille, J. C. (1986). The water vapor budget of the stratosphere studied using LIMS and SAMS satellite data. *Quarterly Journal of the Royal Meteorological Society*, *112*(474), 1127–1143.

Kirk-Davidoff, D. B., Hintsa, E. J., Anderson, J. G., & Keith, D. W. (1999). The effect of climate change on ozone depletion through changes in stratospheric water vapor. *Nature*, *402*, 399–401.

Lambert, A., et al. (2007). Validation of the Aura Microwave Limb Sounder middle atmosphere water vapor and nitrous oxide measurements. *Journal of Geophysical Research*, *112*, D24S36. https://doi.org/10.1029/2007JD008724

Lossow, S., et al. (2018). Trend differences in lower stratospheric water vapour between Boulder and the zonal mean and their role in understanding fundamental observational discrepancies. *Atmospheric Chemistry and Physics*, *18*, 8331–8351.

Lübken, F.-J., Berger, U., & Baumgarten, G. (2018). On the anthropogenic impact on long-term evolution of noctilucent clouds. *Geophysical Research Letters*, *45*. https://doi.org/10.1029/2018GL077719

Nedoluha, G. E., Michael Gomez, R., Allen, D. R., Lambert, A., Boone, C., & Stiller, G. (2013). Variations in middle atmospheric water vapor from 2004 to 2013. *Journal of Geophysical Research: Atmospheres*, *118*, 11,285–11,293. https://doi.org/10.1002/jgrd.50834

Oinas, V., Lacis, A. A., Rind, D., Shindell, D. T., & Hansen, J. E. (2001). Radiative cooling by stratospheric water vapor: Big differences in GCM results. *Geophysical Research Letters*, *28*(14), 2791–2794.

Oltmans, S. J., & Hofmann, D. J. (1995). Increase in lower-stratospheric water vapor at mid-latitude Northern Hemisphere site from 1981 to 1994. *Nature*, *374*, 146–149.

Oltmans, S. J., Vomel, H., Hofmann, D. J., Rosenlof, K. H., & Kley, D. (2000). The increase in stratospheric water vapor from balloonborne frostpoint hygrometer measurements at Washington, D.C. *Geophysical Research Letters*, *27*(21), 3453–3456.

Randel, W. J., Wu, F., Oltmans, S. J., Rosenlof, K., & Nedoluha, G. E. (2004). Interannual changes of stratospheric water vapor and correlations with tropical tropopause temperatures. *Journal of the Atmospheric Sciences*, *2133-2148*.

Randel, W. J., Wu, F., Vomel, H., Nedoluha, G. E., & Forster, P. (2006). Decreases in stratospheric water vapor after 2001: Links to changes in the tropical tropopause and the Brewer-Dobson circulation. *Journal of Geophysical Research*, *111*, D12312. https://doi.org/10.1029/2005JD006744

Remsberg, E., Damadeo, R., Natarajan, M., & Bhatt, P. (2018). Observed responses of mesospheric water vapor to solar cycle and dynamical forcings. *Journal of Geophysical Research: Atmospheres*, *123*(7), 3830–3843. https://doi.org/10.1002/2017JD028029

Rong, P., Russell, J. M., Marshall, B. T., Gordley, L. L., & Mlynczak, M. (2019). Sounding of the Atmosphere using Broad Emission Radiometry (SABER) measured v2.01 water vapor validation. *J. Atmos. Space Terr. Physcs*, *194*, 105099.

Russell, J. M., Mlynczak, M. G., Gordley, L. L., Tansock, J., & Esplin, R. (1999). An overview of the SABER experiment and preliminary calibration results. *Proceedings of SPIE The International Society for Optical Engineering*, *3756*, 277–288.

Shindell, D. T. (2001). Climate and ozone response to increased stratospheric water vapor. *Geo. Phys. Lett.*, *28*(8), 1551–1554.

Smith, C. A., Haigh, J. D., & Toumi, R. (2001). Radiative forcing due to trends in stratospheric water vapour. *Geophysical Research Letters*, *28*(1), 179–182.

Solomon, S., Rosenlof, K., Portmann, R. W., Daniel, J. S., Davis, S. M., Sanford, T. J., & Plattner, G. (2010). Contributions of stratospheric water vapor to decadal changes in the rate of global warming. *Science*, *327*, 1219–1222.

Solomon, S. D., Ivy, J., Kinnison, D., Mills, M. J., Neely, R. R. III, & Schmidt, A. (2016). Emergence of healing in the Antarctic ozone layer. *Science*, *353*, 6296.

Thomas, G. E., Olivero, J. J., Jensen, E. J., Schröder, W., & Toon, O. B. (1989). Relation between increasing methane and the presence of ice clouds at the mesopause. *Nature*, *338*, 490–492.

Wallace, J., & Hobbs, P. V. (2006). *Atmospheric science: An introductory survey*. Academic: Press.

Waters, J. W., et al. (2006). The Earth observing system microwave Limb Sounder (EOS MLS) on the Aura satellite. *IEEE Transactions on Geoscience and Remote Sensing*, *44*, 1075–1092.

Yue, J., Russell, J. III, Jian, Y., Rezac, L., Garcia, R., Lopez-Puertas, M., & Mlynczak, M. G. (2015). Increasing carbon dioxide concentration in the upper atmosphere observed by SABER. *Geophysical Research Letters*, *42*, 7194–7199. https://doi.org/10.1002/2015GL064696